Cell, Vol. 43, 47–57, November 1985, Copyright © 1985 by MIT 0092-8674/85/110047-11 $02.00/0

Localization of the *fushi tarazu* Protein during Drosophila Embryogenesis

Sean B. Carroll and Matthew P. Scott
Department of Molecular, Cellular
and Developmental Biology
University of Colorado at Boulder
Campus Box 347
Boulder, Colorado 80309

Summary

The *fushi tarazu* (*ftz*) gene of Drosophila acts early in embryogenesis to regulate body segmentation. The localization of the *ftz* protein product in embryos was examined using indirect immunofluorescence microscopy. Antibodies were prepared against a β-galactosidase-*ftz* hybrid protein made in E. coli. The *ftz* protein was first detectable in blastoderm-stage embryos as seven stripes of nuclei encircling the embryos transversely. The stripes persist through the early events of gastrulation, but disappear before overt segmentation is visible. The *ftz* protein is expressed a second time in some nuclei of the developing nervous system. In contrast to the early pattern, at the later stage, *ftz* is expressed in each of fifteen metameric subunits of the embryo.

Introduction

The establishment of the segmental body pattern in Drosophila requires the coordinated function of three classes of zygotically active genes early in development (Nüsslein-Volhard and Wieschaus, 1980; Nüsslein-Volhard et al., 1984; Jürgens et al., 1984; Wieschaus et al., 1984). These three classes have been called gap, polarity, and pair-rule loci based on morphological defects that occur in the absence of wild-type gene activity. It is thought that information incorporated into the oocyte by maternally active genes regulates the activity of the zygotic genes to determine the number and orientation of body segments.

One extensively studied pair-rule locus is the *fushi tarazu* (*ftz*) gene of the Antennapedia Complex (ANT-C) (Kaufman et al., 1980; Wakimoto and Kaufman, 1981). Embryos homozygous for null alleles of *ftz* die during embryonic development and have a pattern of pair-wise segmental fusions that result in an embryo with about one-half the normal number of segments. The *ftz* gene has been analyzed molecularly (Weiner et al., 1984; Kuroiwa et al., 1984), and the gene has been sequenced (Laughon and Scott, 1984). The gene has a 1.95 kb transcription unit, the RNA product of which is expressed maximally at 2–4 hr of development. In situ hybridization of *ftz* DNA probes to frozen sectioned embryos revealed that *ftz* transcripts are present in the syncytial blastoderm-stage embryo. The transcripts are localized in a series of well defined stripes that transverse the blastoderm stage embryo even before cell membranes form (Hafen et al., 1984). No *ftz* transcripts were observed in embryos older than 4 hr (Hafen et al., 1984).

To examine the expression and localization of the *ftz*-encoded protein product, the *ftz* protein was produced as a hybrid protein in E. coli. Antibodies specific to the *ftz* portion of this fusion protein were purified. Immunofluorescence analysis of fixed whole-mount embryos was used to study the cellular localization of *ftz* gene product, and the time and site of its expression. We observe that *ftz* protein is located in nuclei in a striped pattern, that not all of the *ftz*-expressing blastoderm stripes are of equal width, that the stripes become narrower during gastrulation, and that *ftz* protein is also detected in the developing ventral nervous system in a pattern quite different from its earlier distribution in the embryo.

Results

Expression of the *ftz* Protein in E. coli

For the generation of antibodies directed against the *ftz* protein, a gene fusion was constructed in λgt11 to produce the protein in E. coli (Young and Davis, 1983). To express *ftz* as a hybrid protein, a 1228 bp Ava II fragment from the pDmG20 *ftz* cDNA (Laughon and Scott, 1984), with appropriate Eco RI linkers ligated to it, was introduced into the Eco RI site of λgt11 (Figure 1). The phage (λ*ftz*A10) produces a hybrid protein containing 399 amino acids of *ftz* protein and lacking only the five N-terminal and nine C-terminal amino acids of the deduced *ftz* product (Laughon and Scott, 1984).

Lysogens containing the λ*ftz*A10 phage were induced to express the hybrid β-galactosidase-*ftz* hybrid protein. Upon thermal induction a fusion protein migrating with an apparent molecular weight of 175 kd was produced (Figure 2A). The protein migrates more slowly than expected from the known sequence (160 kd is predicted). The high proline content (10%) of *ftz* may be responsible for the anomalous migration of the hybrid protein. The induced protein was indeed a hybrid; it reacted with both anti-β galactosidase antibody (Figure 2B) and with an antibody against a synthetic 11 amino acid oligopeptide (Carroll et al., 1985) corresponding to the N-terminal part of the *ftz* homeodomain (Figure 2C). Anti-homeodomain antiserum reacted more strongly with a slightly faster migrating band, presumably a degradation product of the full-length fusion protein, perhaps caused by protein conformation effects.

Antibodies against *ftz* Protein

Antiserum for use in immunofluorescence studies was elicited by immunization with *ftz*-βgal fusion protein purified using amino-phenyl thiogalactopyranoside affinity chromatography (see Experimental Procedures). The immune serum was affinity-purified using hybrid protein cross-linked to anti-β-galactosidase antibody attached to Sepharose 4B. The specificity of the final antibody prepa-

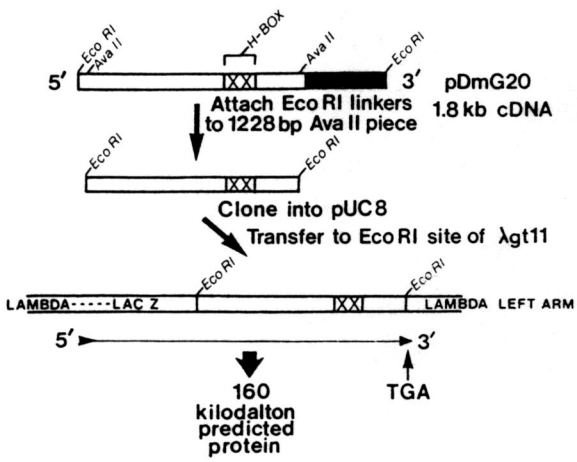

Figure 1. Construction of *lacZ-ftz* Gene Fusion in λgt11

An Ava II subclone of the *ftz* pDmG20 cDNA (Laughon and Scott, 1984) was inserted into pUC8 at the unique Eco RI site using 10 bp (CGGAATTCCG) Eco RI linkers ligated to the 1228 bp coding fragment of *ftz*. H-BOX, the 180 bp homeobox sequence. The subcloned, linkered fragment was then transferred, in the proper orientation, into the unique Eco RI site of the λgt11 expression vector (see Experimental Procedures).

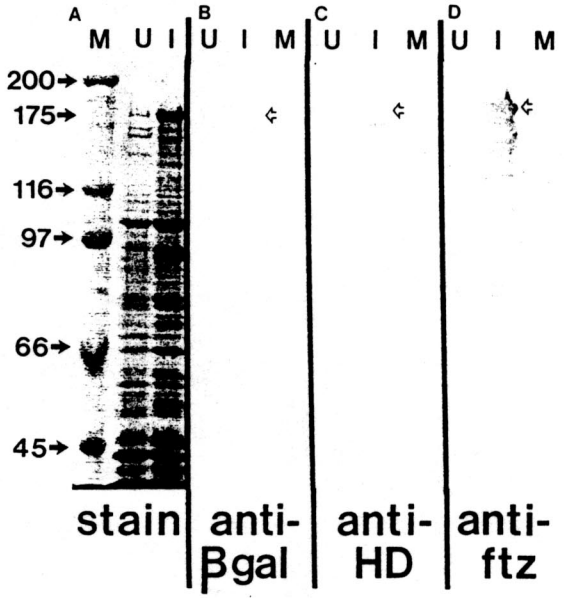

Figure 2. Expression of a β-galactosidase-*ftz* Fusion Protein in E. coli and Production of Specific Antibodies to the *ftz*-Encoded Domain

Lysogens were grown for 2 hr at either 30°C (uninduced) or 42°C (induced), and cell lysates were prepared for electrophoresis on a 7.5% SDS-polyacrylamide gel. Part of the gel was stained with Coomassie blue (A), and replicate lanes were transferred to nitrocellulose and were probed with affinity-purified antibodies against: β-galactosidase (B); an 11 amino acid peptide of the homeodomain (C); or the *ftz* portion of the hybrid protein (D). The molecular weight markers indicated in A are myosin (200 kd), β-galactosidase (116 kd), phosphorylase b (97 kd), bovine serum albumin (66 kd), and ovalbumin (45 kd). The arrows indicate the position of the full-length hybrid protein (migrating as 175 kd). Note that a small amount of hybrid protein is present in uninduced cultures because of the absence of repression in strains without *lac* I^q. Many antigenic degradation products are present in induced cells. U, uninduced; I, induced; M, markers.

ration for the *ftz*-encoded portion of the fusion protein was demonstrated using protein blots (Figure 2). The affinity-purified antibody reacted with *ftz* fusion protein but not with β-galactosidase or other E. coli proteins. The larger number of anti-*ftz* labeled bands were presumably because of the presence of breakdown or prematurely terminated products of the hybrid protein. To localize *ftz* antigen during embryogenesis, whole fixed embryos were stained with anti-*ftz* antibodies according to the method of Mitchison and Sedat (1983).

Expression of *ftz* during Embryogenesis

After fertilization, the Drosophila embryo undergoes a series of nearly synchronous nuclear divisions (Foe and Alberts, 1983). At about the eighth nuclear division the nuclei begin to migrate to the periphery of the embryo, a ninth division takes place enroute, and the nuclei undergo four more divisions in the cortical region of the egg. It is after the eleventh nuclear division that *ftz* mRNA is first clearly detectable by in situ hybridization to sectioned embryos. The striped distribution of *ftz* transcripts appears at about the time of the thirteenth division (Hafen et al., 1984).

In control experiments, wild-type embryos were stained with antibodies against the β-galactosidase portion of the *ftz* hybrid protein (Figures 3a and 3b) and homozygous mutant embryos, ftz^{w20}/ftz^{w20}, which presumably lack *ftz* product (Weiner et al., 1984) were stained with the anti-*ftz* antiserum (Figure 7c). In both cases, no specific staining was observed at any developmental stage examined.

Immediately after the thirteenth nuclear division, no localized immunofluorescent labeling was detected with anti-*ftz* antibodies (Figures 3c and 3d). However, by the cellular blastoderm stage, some 30 min after the last nuclear division, *ftz* protein was detected within nuclei in a pattern of seven stripes, each about four nuclei wide in the anterior–posterior axis (Figures 4a and 4d). Therefore, the *ftz* protein becomes detectable during the time between the last nuclear division and the beginning of gastrulation. During this 30 min interval, no cell divisions take place (Hartenstein and Campos-Ortega, 1985). At all stages, faint staining of all nuclei is seen in addition (Figure 4, Figure 5, and Figure 6); such general nuclear staining is not seen with control sera (not shown). The most posterior stripe appears slightly wider than the others, averaging about five nuclei across. The spaces between the stained stripes are about four nuclei wide. At the beginning of gastrulation, the stripes become narrower, averaging three nuclei across, except for the most posterior stripe that remains about five nuclei wide. At the same time, the spaces between the stripes increase to a width of about five nuclei. In some preparations, it is possible to see the stripes extending around the embryo (Figure 4c). Note that since the nuclei are hexagonally close-packed, the number of nuclei spanning a stripe (or space) is not integral, and the numbers are therefore approximate.

As gastrulation begins, the mesodermal precursor cells move into the interior of the embryo through the ventral furrow (Figures 4b and 4e). Cells moving into the furrow were stained, in the striped pattern, by the anti-*ftz* antibod-

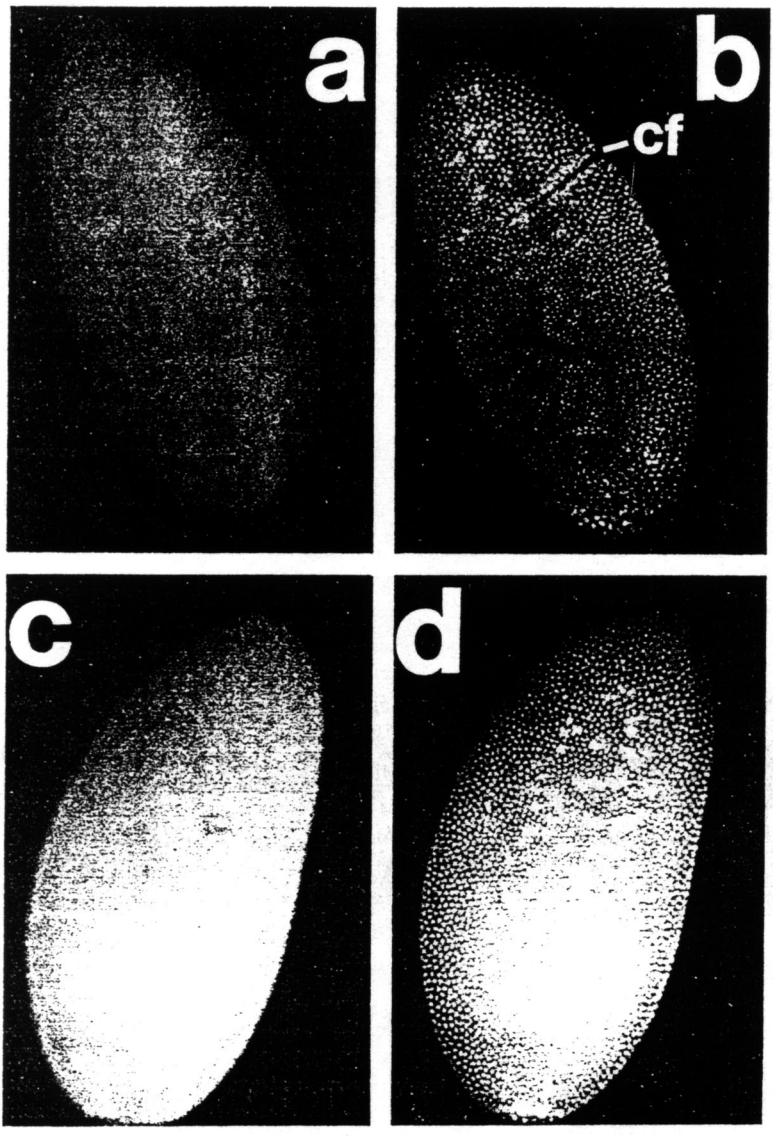

Figure 3. Control and Early Staining Patterns

Antibodies against β-galactosidase were affinity-purified from serum from the same rabbit from which the anti-*ftz* antibodies were prepared. (a) The immunofluorescent staining of an embryo in the early stages of gastrulation, stained (as in Experimental Procedures) with anti-β-galactosidase. (b) The same embryo as in a, stained with the DNA-marking dye, DAPI. cf, cephalic furrow. (c and d) Upon the completion of the thirteenth nuclear division, cell membranes begin to form around the nuclei. (c) Embryos later than the thirteenth nuclear division stained with anti-*ftz* antibodies. (d) Same embryo as in c, stained with DAPI.

ies. The most anterior stripe is located just posterior to the cephalic furrow, although the stripe and the furrow do not precisely align at all times (Figure 5a). As gastrulation proceeds, the stripes become wedge-shaped, about two to three nuclei wide on the dorsal side, and about four nuclei wide ventrally (Figures 5a and 5d). The posterior stripe remains the widest and is also somewhat wedge-shaped. These changes appear to be due to rearrangements of cells, although we cannot rigorously eliminate the possibility that a different subset of the cells begins to produce *ftz* antigen. After formation of the furrows, the germ band, a ventral strip of ectodermal cells in which segments will first become visible, begins to form and to extend around the posterior end of the embryo. The lengthening of the germ band is thought to be due largely to cell movement rather than to cell division (Sander, 1976; Hartenstein and Campos-Ortega, 1985).

The indentation that will become the posterior midgut invagination begins to form posteriorly to the posteriormost stripe (the flattened posterior end in Figure 5b), while the first signs of the posterior transverse fold (pf in Figure 5b) appear dorsally at the location of the stripe fifth from the anterior. The stripes can still be seen dorsally and ventrally as the pole cells enter the posterior midgut invagination (Figures 5c and 5e). Parts of the fourth and fifth stripes disappear into the posterior transverse fold. Eventually part of the sixth stripe is drawn into the fold as well, at a time after the pole cells have completely disappeared into the posterior midgut invagination (Figure 6a). The posterior end of the embryo moves dorsally and then anteriorly during the germ-band elongation phase of development (Poulson, 1950; Turner and Mahowald, 1977). During elongation, the *ftz* stripes can be followed until nearly the time of full germ-band extension (not shown). As the germ band extends, *ftz* expression decreases in the dorsolateral cells while remaining present in the germ band. The stripes disappear before the germ band is fully extended.

While the germ band is at its maximum extension, a dramatic change in the pattern of staining occurs. Concomi-

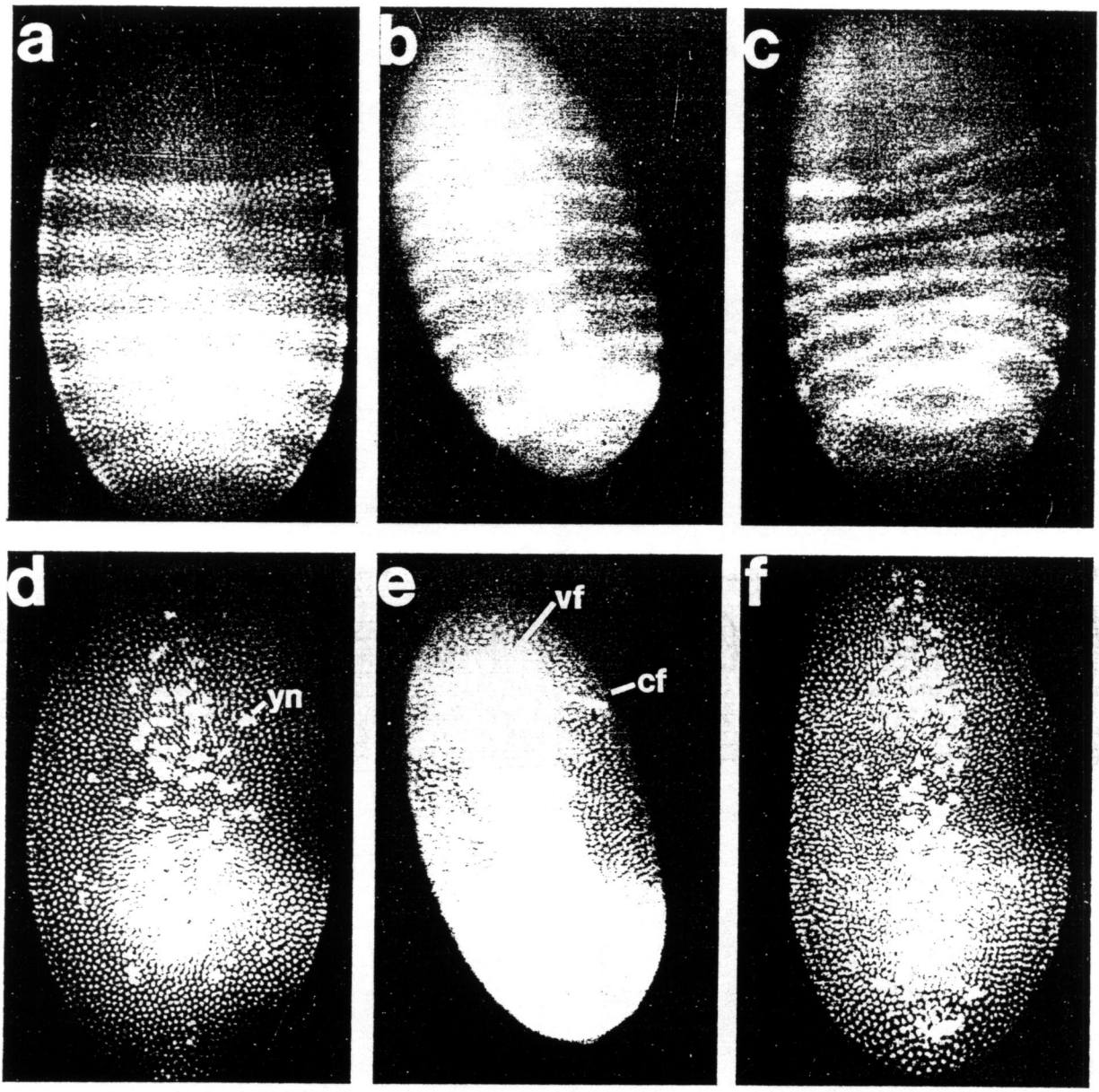

Figure 4. Blastoderm and Early Gastrulation Stage Embryos

In each micrograph, the anterior end of the embryo is at the top. (a, b, and c) Whole-mount embryos incubated with anti-*ftz* antibodies and secondarily stained with fluorescein-conjugated goat anti-rabbit antibody. (d, e, and f) The same three embryos as in a, b, and c (respectively) stained with DAPI. (a and d) An embryo at the cellular blastoderm stage, just beginning gastrulation movements. The large internal bright spots in d are the yolk nuclei. One yolk nucleus is indicated (yn). (b and e) An embryo (ventral view) that has begun gastrulation. The ventral furrow (vf) through which the mesodermal cells move into the interior and the cephalic furrow (cf) are visible. By this stage, the stripes of stained nuclei have narrowed to an average three-cell width, except for the most posterior stripe, rather than the initial four-cell width seen in a. (c and f) A dorsal view of a gastrulating embryo. The immunofluorescent stripes (in c) can be seen to encircle the embryo. As cells move from the dorsal and lateral regions toward the ventral side, the stripes take on a wedge-shaped appearance.

tant with the appearance of the ectodermal invaginations that form tracheal pits, detectable antigen appears in fifteen clusters of germ-band nuclei within the dividing cells of the developing nervous system (Poulson, 1950; Lehmann et al., 1983). From a lateral view, it can be seen that the initial staining is in one cell layer (not shown). From a ventral or dorsal perspective, the earliest staining is of nuclei arranged in a chain of linked hexagons (Figure 6b). The laterally extended vertices of the hexagons are just posterior to the tracheal pits and are also in the approximate positions where the clusters of nuclei staining with anti-*ftz* subsequently coalesce. The clusters (Figure 6c) remain visible during germ-band shortening (Figure 6d). The staining is repeated bilaterally in each of fifteen segmental units, including the regions where the gnathocephalic segments are forming (Figure 6e and Figure 7a). To assess whether this unexpected spatial and temporal pattern of anti-*ftz* staining is caused by the bona fide gene

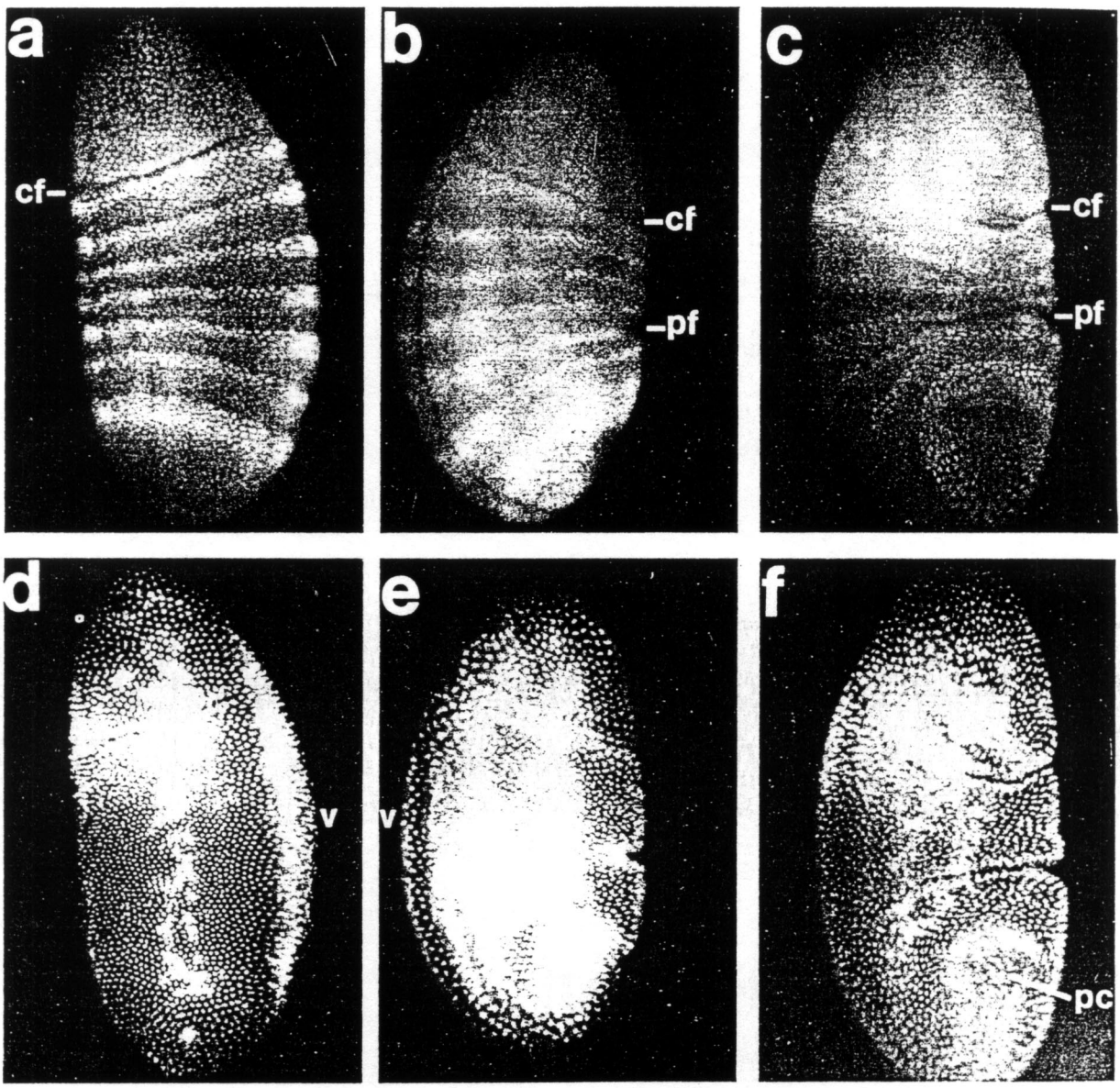

Figure 5. Embryos during Gastrulation

a and d: (a) A dorsolateral view of an embryo showing the anterior stripe of stained nuclei just posterior to the cephalic furrow (cf). (d) DAPI-stained image of same embryo as in a. The distorted shape of the nuclei along the ventral (v) side is associated with the movement of the cells in that region into the ventral furrow.

b and e: (b) A lateral view of an embryo in which the posterior transverse fold (pf) is beginning to form. The indentation at the posterior (bottom) end is the beginning of the posterior midgut invagination. The cephalic furrow (cf) is still visible. The ventral furrow is visible by both immunofluorescent staining, and by the DAPI staining (in d), along the ventral (v) side.

c and f: A dorsolateral view of an embryo that is beginning germ-band elongation. (c) Most of the posterior endoderm has moved into the posterior midgut invagination, leaving the double-width stripe of *ftz* protein near the posterior end. The cephalic furrow (cf) and posterior transverse fold (pf) are visible. (f) The pole cells (pc) are in the process of entering the posterior midgut invagination in this embryo. Some of the cells around that invagination are distorted in shape as they bend into the opening. Most of the cells that contain detectable *ftz* protein are not distorted in this way (compare c and e).

product, we examined homozygous mutant ftz^{w20} embryos for staining. The ftz^{w20} allele has a 5 kb transposon inserted into the protein-coding sequence of the gene (Weiner et al., 1984). Staining of the neural cells was not detectable at any stage of mutant embryo development (example in Figures 7c and 7d). Therefore, the neural staining is indicative of either authentic *ftz* protein product or a cross-reactive protein that requires ftz^+ function for its expression. The fifteen-unit staining pattern disappears shortly after germ-band shortening is completed (Figure 7b), and no staining with the anti-*ftz* serum is seen at later embryonic stages (data not shown).

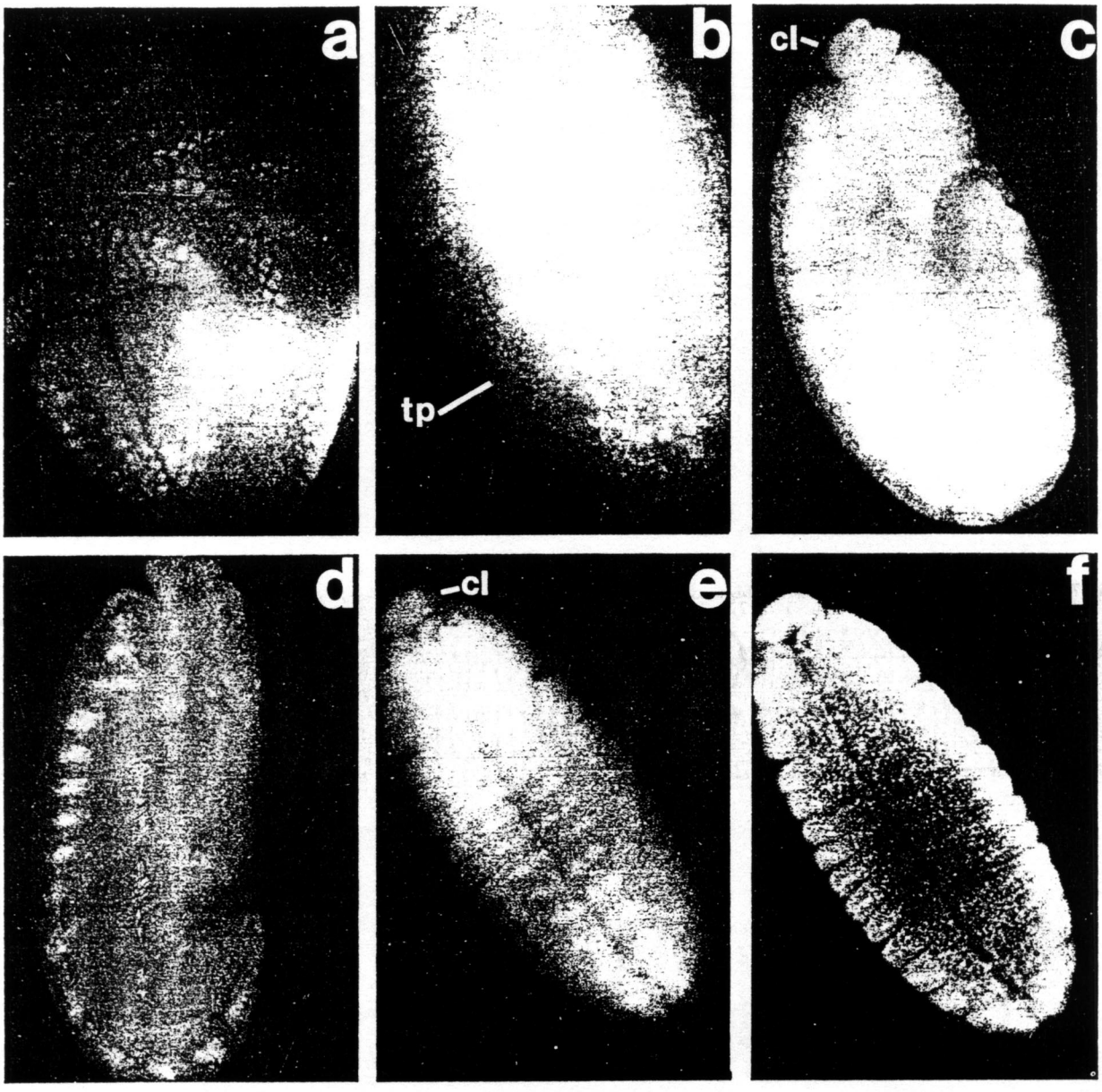

Figure 6. Protein Patterns Later in Embryogenesis

(a) A dorsal view of the posterior end of an embryo. The pole cells have moved into the interior. The *ftz* staining is beginning to lose intensity. The fourth, fifth, and sixth stripes merge in the posterior transverse fold. (b) A ventral view of an embryo with an elongated germ band, stained with anti-*ftz*. The tracheal pits (tp) are visible. The first detectable antigen is arranged in linked hexagons. The antigen is in the nuclei. (c) Lateral view of an embryo with an elongated germ band, stained with anti-*ftz*. The clypeolabrum (cl) marks the anterior end of the embryo. Fifteen units of staining are visible. (d) Same as c, but during germ-band shortening. (e) Ventral view of an embryo near the end of germ-band retraction. The clypeolabrum (cl) is at the anterior end of the embryo. Antigen is visible in all of the subdivisions of the germ band and is located in patches flanking the ventral midline. (f) DAPI-stained view of the embryo shown in e.

Discussion

The *ftz* Protein Accumulates in Embryonic Nuclei

The molecular functions of proteins encoded by segmentation genes and homeotic genes are unknown. Based on structural homology between part of the homeodomain and bacterial DNA-binding proteins, it has been hypothesized that one function of the family of homeodomain-containing proteins is to bind to DNA (Laughon and Scott, 1984). The nuclear location of the *ftz* protein is consistent with this hypothesis. Two other Drosophila homeodomain-containing proteins have been localized in both embryonic and imaginal disc nuclei, the *Ultrabithorax* protein (White and Wilcox, 1984; Beachy et al., 1985), and the *engrailed* protein (Di Nardo et al., 1985). Other genes containing homeoboxes include the homeotic genes *Antennapedia*, *Sex combs reduced*, *Deformed*, *infraabdominal-2*, and *infraabdominal-7* (Scott and Weiner, 1984;

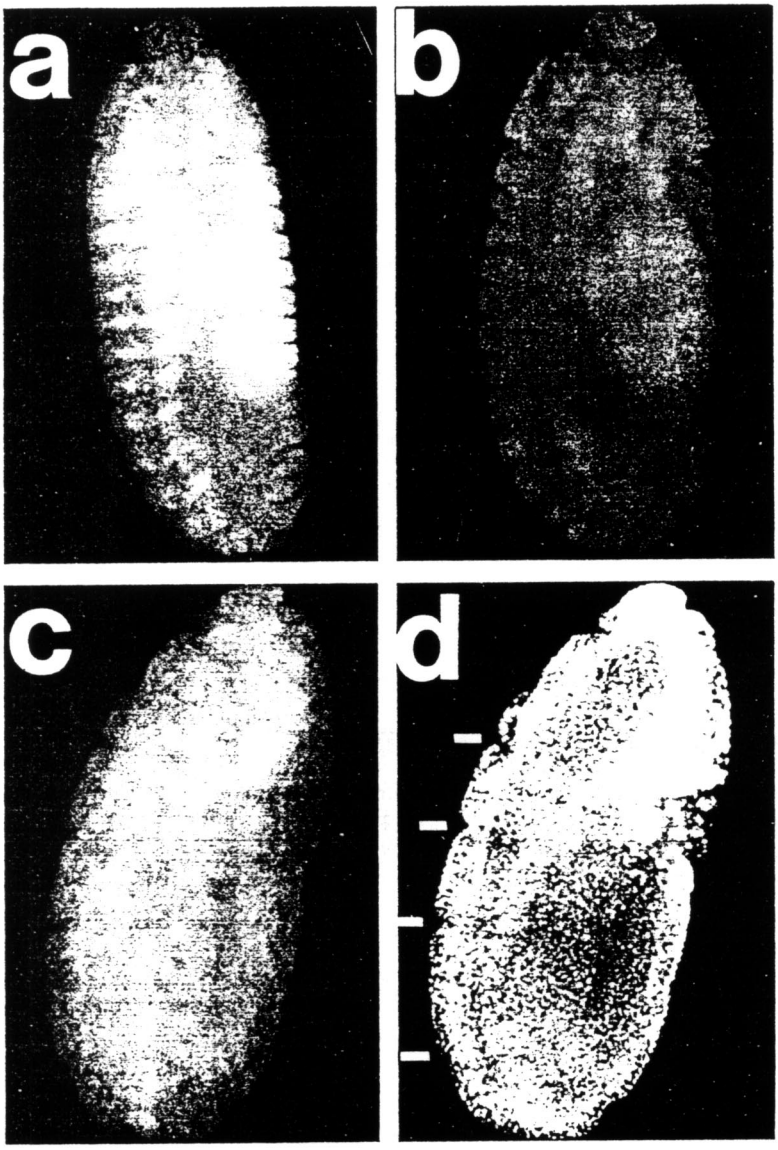

Figure 7. Protein Patterns after Germ-Band Shortening and in *ftz*⁻ Embryos

(a) Ventrolateral view of embryo stained with anti-*ftz* at the end of germ-band shortening. The light patch seen at the right (dorsally) is in the region of the remaining yolk and is not due to immunofluorescence. (b) Ventrolateral view of an embryo at a slightly later stage than the embryo in a. The ventral staining with anti-*ftz* has disappeared. (c and d) Immunofluorescent (c) and DAPI (d) staining of an embryo after germ-band shortening. The embryo has about half the usual number of body divisions because it is homozygous for a *ftz* null mutation (ftz^{w20}/ftz^{w20}). No immunofluorescent staining of embryos of this genotype (recognized by their diminished segment number) is observed. The bars in d indicate the remaining body divisions.

McGinnis et al., 1984; Gehring, 1985; Laughon, Storfer and Scott, unpublished observations). The products of these genes may well also be located in nuclei.

The Arrangement of Segmental Precursor Cells

The analysis of whole-mount embryos with *ftz* protein-specific antibody allows the detection of *ftz* protein up to the 10 hr stage of embryogenesis; *ftz* mRNA has been detected only up to about the four and a half hr stage (Hafen et al., 1984). When the *ftz* protein is first detected, the stripes of immunofluorescent labeling are about four nuclei wide, in the anterior–posterior axis. A precise number cannot be determined because the nuclei are arranged (approximately) in a hexagonally close-packed array. Also, at the edges of each stripe, some nuclei appear to stain weakly. At the edges of the embryo where the signal is strongest because of vertical stacking of stained nuclei (Figures 4a and 4b), four stained nuclei appear to alternate with four unstained nuclei.

As gastrulation begins, the *ftz* stripes become narrower, averaging three nuclei across instead of four. The rapid disappearance of *ftz* protein from some of the blastoderm nuclei suggests that a specific mechanism for elimination of the protein may exist. Later still, the stripes become wedge-shaped, averaging two nuclei wide dorsally and four nuclei wide ventrally. The most posterior stripe appears slightly wider than the other stripes at the blastoderm stage (Figure 4a) and does not become distinctly narrower during early gastrulation movements (Figure 5). As a result, during gastrulation the posteriormost stripe remains about twice as wide as the others.

The identity and number of segments at the posterior end of Drosophila is a matter of some uncertainty. Most primitive insects have eleven abdominal segments plus a terminal segment, while Drosophila have only eight obvious segments. The double-width posterior *ftz* stripe may be due to the evolutionary disappearance of one or more segments that in more primitive insects would divide the

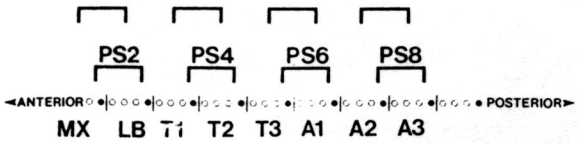

Figure 8. Diagram of a Model for the Blastoderm-Stage Segmental Primordial Cells

The blastoderm cells are represented in a lateral view as repeating segmental primordia, each four cells wide in the anterior–posterior axis. Only part of the embryo is represented. The cells that will form posterior compartment structures are shown as filled circles; cells that will form anterior compartment structures are shown as open circles. The segments (maxillary, labial, first, second, and third thoracic, and first, second, and third abdominal) and some of the parasegments (lower brackets; PS 2, 4, 6, and 8) are indicated. The two rows of brackets indicate two possible frames in which the *ftz*$^+$ protein might be expressed when it first appears in four-cell wide stripes at the cellular blastoderm stage. In *ftz*$^-$ embryos, the segment boundaries between MX and LB, T1 and T2, T3 and A1, A2 and A3, and so on, fail to form. Therefore, we have indicated two frames that straddle the segment boundary and are consistent with the pattern elements deleted when *ftz*$^+$ is absent.

double-width *ftz* stripe. Perhaps the "lost" segments are the eighth, tenth, and eleventh, and the seventh and ninth segments remain, fused together.

It has been estimated that the precursor cells for each segment lie in a band three to five cells wide at the blastoderm stage (Lohs-Schardin et al., 1979). The *ftz* results are consistent with this estimate, although the *ftz* stripes may not correspond to segmental primordia. If the blastoderm-stage repeating units are four cells wide, then there are at least four "phases" in which the cells can be grouped. One repeating unit would be segmental, units of an anterior compartment plus a posterior compartment. Another phase would give parasegments (Martinez-Arias and Lawrence, 1985), units of a posterior compartment plus an anterior compartment. The difference between a segment and a parasegment is only a frameshift of one cell (Figure 8), since the posterior compartment is likely to be only one cell wide (Kornberg et al., 1985; DiNardo et al., 1985). The remaining two possible phases each consist of one posterior compartment primordium plus parts of each of two anterior compartment primordia (Figure 8).

The striped pattern of the *ftz* protein does not endure long enough to decide in what phase *ftz* is expressed. One argument supporting a nonsegmental unit as the correct phase of *ftz* expression comes from the *ftz*^{Rpl} allele (Laughon and Scott, 1984), which causes a homeotic transformation of the posterior compartment of metathorax (T3) into mesothorax (T2). Only if *ftz*$^+$ is expressed in a nonsegmental phase would posterior T3 be a site of *ftz* expression (Figure 8). It has not been demonstrated, however, that the *ftz*^{Rpl} allele is expressed in only the same places as *ftz*$^+$. It is known that the *ftz*^{Rpl} allele encodes an altered protein, which we suggested may interfere with bithorax complex function to cause the homeotic transformation (Laughon and Scott, 1984). The *engrailed* (*en*) protein, which is likely to be an indicator of posterior compartments of the segments (Kornberg, 1981), is first detected slightly later than *ftz* (DiNardo et al., 1985), in stripes averaging one nucleus in width. The use of *en* and *ftz* probes together may help to resolve the issue of the phasing of *ftz* expression.

Two important facts make the oversimplified models described here only approximations: blastoderm nuclei are not arranged in neat rows, they are hexagonally close-packed, and, second, the demarcation between staining and nonstaining nuclei often does not appear to be abrupt, some nuclei appear to stain weakly. Both of these observations suggest that the expression of *ftz* may be controlled by an underlying system of continuous gradients, and that the sharp borders that eventually form (for example between compartments) may be due to a "focusing" process dependent on the expression of *ftz* itself and other interacting genes.

Other pair-rule genes, such as *hairy*, *even-skipped*, *odd-skipped*, *paired*, and *odd-paired* may be expressed with different phasing with respect to *ftz*, *engrailed* and each other. Homeotic genes such as *Antp* and *Ubx* could also be expressed in different phases. In this way, the combinatorial action of the genes can be envisioned to specify the identity of each cell as a function of its relative position within the repeating units of the embryo. The lack of coincidence between the borders of the embryo regions affected by pair-rule segmentation gene mutations and the segmental (or compartmental) boundaries was noted when the effects of the genes were first described (Nüsslein-Volhard and Wieschaus, 1980), which suggested that the genes can operate in frames other than compartmental ones. By acting in different phases, some of the early acting segmentation loci may be the determining factors in defining the polyclones that will form the compartmental lineage units (Garcia-Bellido, 1968; Crick and Lawrence, 1975). The *ftz* antibody probe provides precise landmarks along the embryo with which the relative phasing of the expression of other pair-rule gene products can eventually be assessed.

ftz and the Ventral Nervous System

One of the unexpected results of the in situ hybridization of homeotic gene DNA probes to the RNA of sectioned embryos was the high concentration of transcripts in the nervous system. Both *Ultrabithorax* (Akam, 1983) and *Antennapedia* (Levine et al., 1983) transcripts are located in specific parts of the ventral ganglia. In contrast to these homeotic genes, segmentation genes such as *ftz* and *engrailed* have not been reported to have major accumulations of transcripts in neural cells (Hafen et al., 1984; Kornberg et al., 1985). It was therefore a surprise to find a nuclear protein in parts of the nervous system that is recognized by the anti-*ftz* serum (Figure 6).

There are several possible explanations for the neural staining. First, the staining may be due to authentic *ftz* protein. The *ftz* RNA may be at a low level in the nervous system and may have been missed. Some recent in situ hybridization analyses of sectioned embryos with *ftz* probes have detected transcripts in neural tissue in a pattern similar to that reported here for *ftz* protein (M. Levine, personal communication). Northern blot analysis of staged embryonic RNA indicated that *ftz* mRNA is detect-

able up to 10–12 hr of development, although at a lower level than its expression at cellular blastoderm (Weiner et al., 1984). The absence of the neuroblast staining in *ftz*⁻ embryos is consistent with the signal being due to *ftz*-encoded protein, but another possibility is that the antiserum cross-reacts with one or more proteins the expression of which requires *ftz*⁺ function. A third possibility is that only part of the observed staining is due to authentic *ftz* protein, for example, that found in alternate segments.

One likely source of cross-reactivity would be the 60 amino acid *ftz* homeodomain structure that is shared with several other proteins. However, the antiserum against *ftz* contains only a very low level of reactivity with other homeodomain-containing proteins, as assayed by protein blotting (Carroll and Scott, unpublished observations). Furthermore, the transient position-specific signal observed with anti-*ftz* antibody is not consistent with the previously described patterns of homeotic gene transcription in the nervous system (Akam, 1983; Levine et al., 1983; McGinnis et al., 1984). Also, an antiserum made against a synthetic peptide representative of part of the homeodomain reacts with nuclei from most or all parts of the embryo as well as all nuclei in the nervous system (Carroll et al., 1985). The faint staining of all nuclei seen with the anti-*ftz* serum might be accounted for by homeodomain cross-reactivity. Experiments to identify on blots the proteins detected by the *ftz* antibodies have not yet succeeded convincingly, and we do not know the number of forms of the native *ftz* protein or of any cross-reactive polypeptides.

The expression of *ftz* in the nervous system raises the question of a late function for the product. In an analysis of the temperature-sensitive period of a *ftz* ts allele (Wakimoto et al., 1984), the major period of sensitivity was from 2 to 4 hr of development, at the blastoderm stage. However, in addition, some lethality was observed if mutant embryos were shifted to the restrictive temperature as late as 6 or 8 hr into development. These data provide a hint that *ftz* may function later than blastoderm stage. It is also possible that lack of *ftz* function in the nervous system does not cause much lethality, or that prior function of *ftz* in neuroblasts at the early stages of gastrulation partially protects embryos from a subsequent loss of *ftz* function. Clonal analysis has shown that no *ftz* function is required for differentiation of adult cuticular structures later than 12 hr of development (Wakimoto et al., 1984). *ftz* mRNA is not detectable after 12 hr of development (Weiner et al., 1984). The distinct temporal and spatial patterns of *ftz* expression in the ectoderm and neural tissues suggests that the regulation of the *ftz* gene expression is more complex than was previously thought. The identification of those genes influencing *ftz* expression at each stage of development and the elucidation of *ftz* function at the cellular and molecular level remain the most pressing issues for eventually understanding the role of this pair-rule gene in Drosophila embryonic pattern formation.

Experimental Procedures

Gene Fusion

The *ftz* cDNA clone pDmG20 has been described previously (Weiner et al., 1984; Laughon and Scott, 1984). A 1228 bp Ava II fragment containing nearly all of the coding region was purified, its recessed 3′ termini filled in with the Klenow fragment of E. coli DNA polymerase, and Eco RI 10-mer linkers (New England Biolabs) that had been phosphorylated with T4 polynucleotide kinase were ligated to the now blunt-ended Ava II fragment. After ligation, the DNA was digested with Eco RI, and the fragment was purified. To amplify the fragment and remove tandem linkers, it was cloned into pUC8, the purified plasmid DNA was digested with Eco RI, and the 1.2 kb Eco RI fragment was purified on a preparative gel. The fragment was then ligated into Eco RI-digested λgt11 (Young and Davis, 1983) at the unique site near the 3′ end of the *lacZ* gene. The phage were packaged, plated on RY1090, and scored for colorless plaques. The DNA from plaque-purified phage was prepared and screened for insertion of the *ftz* fragment in the proper orientation.

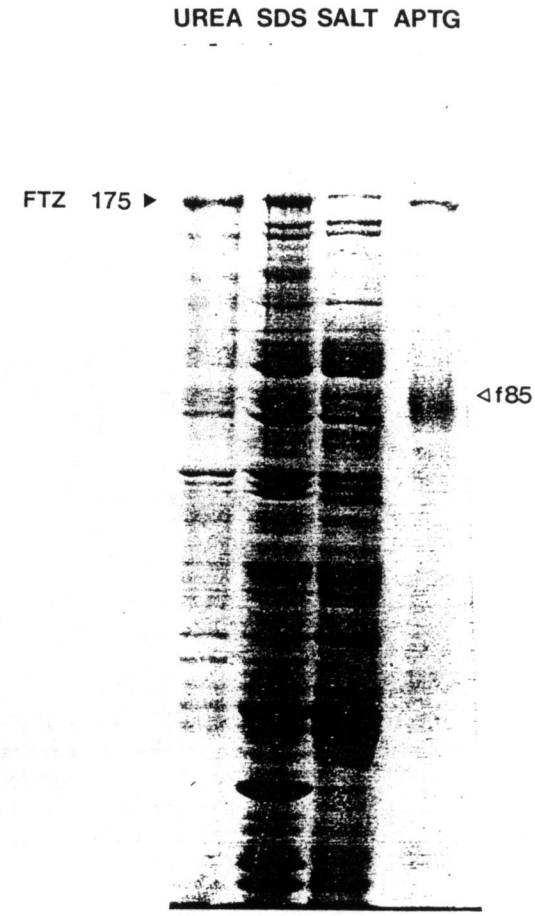

Figure 9. Extraction and Purification of the β-galactosidase-*ftz* Hybrid Protein

Hybrid protein to be used as an immunogen was extracted with 8 M urea, 1.5% SDS, or 50 mM $NaPO_4$. The protein in the extract was further purified on APTG-Agarose. The equivalent of 200 μl of original culture volume of each extract was applied to a 7.5% SDS-polyacrylamide gel and was stained with Coomassie blue. The APTG-purified material contains mostly intact hybrid protein (denoted by arrow at 175 kd) and a β-galactosidase degradation fragment (85 kd).

Expression of Hybrid Proteins

Lysogens of λgt11-*ftz* Av10 were established in RY1089. The pMC9 plasmid carrying the *lac* I^q gene was cured from the strain to permit optimal induction. (Even at 10 mM IPTG, induction of hybrid protein is not as efficient as when no *lac* I^q repressor gene is present.) A culture of the lysogen was grown at 30°C overnight in NZCYM to saturation and then was diluted 1/100 and grown to a density of 4×10^8 cells/ml at 30°C. To induce the production of hybrid protein, the culture was

shifted to a 45°C waterbath for 15 min. After 2 hr at 37°C, cells were harvested by centrifugation and solubilized in 1.5% SDS-polyacrylamide gel sample buffer in 1/10 of the original cell culture volume and then heated for 5 min at 100°C. Lysates were clarified by centrifugation for 5 min in an Eppendorf centrifuge, and 25 μl of the supernatant was loaded per lane onto an analytical 7.5% SDS-polyacrylamide gel (Weber and Osborn, 1975).

Purification of Hybrid Proteins

The β-galactosidase-*ftz* Av10 fusion protein was purified by several methods. First, to obtain pure protein in soluble form, it was extracted and purified by aminophenylthiogalactopyranoside-agarose (Sigma) affinity chromatography (Germino et al., 1983). About 1 mg of intact protein per liter of induced culture was obtained in this fashion. About 90% of the fusion protein was not extracted by the above method, but could be solubilized in a buffer containing 8 M urea (Figure 9). The fusion protein from the urea extract, after dialysis, was purified using either anti-β-galactosidase antibody columns (see below) or preparative SDS-polyacrylamide gels. By a combination of these methods, mildly treated or denatured protein was purified for use as an immunogen in amounts ranging from 1–10 mg per liter of induced culture. Additional information on these and the methods below are available as detailed protocols upon request.

Production, Purification, and Assay of Antibodies

Rabbits were immunized with 500 μg of antigen in complete Freund's adjuvant on day 0 and again with 200 μg on days 14 and 21 (and monthly thereafter) in incomplete adjuvant. All injections were subcutaneous at multiple sites. Immunizations with gel-purified SDS-denatured antigen (200 μg each) were intramuscular in incomplete Freund's adjuvant. Rabbits were bled on day 28 and about monthly thereafter until the final exsanguination.

Sera were absorbed to remove anti-β-galactosidase antibody by repeated passages on β-galactosidase-Sepharose 4B. The resin was made by coupling 1 mg of enzyme per ml of CNBr-activated resin. The columns were loaded with 5–20 ml of serum, washed with phosphate-buffered saline (PBS), BBS-Tween (0.1 M boric acid, 25 mM sodium borate, 1 M NaCl, and 0.1% Tween 20) and PBS again. The bound antibody was eluted with 4 M Guanidine-HCl, 10 mM Tris (pH 8.0), and the eluate was dialyzed against PBS overnight.

The flow-through fraction of the β-galactosidase column was fractionated on an anti-β-galactosidase-DMP-*ftz* Av10 affinity column as follows: the column was prepared by attaching 1 mg of affinity-purified anti-β-galactosidase antibody per ml of CNBr-activated Sepharose 4B. A dialyzed urea extract containing 1 mg/ml of intact fusion protein was then passed over the column. The column was washed, until the effluent was free of protein, with PBS, BBS-Tween, PBS, and 0.2 M triethanolamine (pH 8.2). To attach the fusion protein covalently, the column beads were suspended in 10 vol of 0.2 M triethanolamine, 50 mM dimethylpimelimidate-2 HCl and adjusted to pH 8.2. The antibody–antigen complexes were cross-linked by rocking the beads gently in this solution at room temperature for 45 min (Schneider et al., 1982). The beads were poured into a column and washed with PBS, noncovalently bound protein was removed with 4 M Guanidine-HCl washes, and the column was equilibrated in PBS. The serum from which anti-β-galactosidase antibodies had been removed was then applied, the column was washed as above, and the eluted antibody was dialyzed against PBS. The purified antibody was passed once more over the β-galactosidase column, to remove residual contaminating anti-β-galactosidase antibodies in order to obtain the final anti-*ftz* antibody.

The specificity of purified antibody was tested on proteins resolved by PAGE and transferred to nitrocellulose (Towbin et al., 1979) from lysogen extracts and from purified proteins by incubating a blot with primary antibody (1 μg/ml) for 2 hr, washing with PBS, BBS-Tween, and PBS, and then incubating the blot with affinity-purified alkaline phosphatase-conjugated goat anti-rabbit IgG (Cappel). After washing, the color was developed with bromo-chloro indolyl phosphate and nitro blue tetrazolium at pH 9.5 in 50 mM Na_2CO_3.

Immunofluorescence

Whole Drosophila embryos were dechorionated, permeabilized in heptane, fixed in formaldehyde, and devitellinized in heptane/methanol according to Mitchison and Sedat (1983) as modified by Tim Karr (personal communication). After rehydration, the embryos were treated to block protein-reactive sites with PBS-1% BSA containing 0.1% (vol/vol) of Triton X-100 (PBT) for 3 hr at 4°C. The embryos were incubated overnight at 4°C with agitation in a solution of purified antibodies (1–2 μg/ml) diluted in the PBT buffer. After the primary incubation, the embryos were washed for 3–4 hr with 5–6 changes of PBT. Goat anti-rabbit IgG-FITC, which had been previously incubated with fixed embryos, was diluted 1:500 in PBT. The embryos were incubated in the secondary antibody for 3 hr. The embryos were washed as above, stained with 50 ng/ml diamidino-phenylindole (DAPI) for 3 min, and washed for 30 min more. The embryos were mounted in Tris buffer containing 4 mM ascorbic acid under a coverslip and were viewed by epifluorescence microscopy. Photography was with Kodak Tri-X film used at ASA 1600 and developed in Diafine (Acufine, Inc., Chicago, IL).

Acknowledgments

We thank Dr. Allen Laughon for his continued interest in, and enthusiasm for, all phases of this project, Robert Laymon for superb technical assistance, and Drs. Steven DiNardo and Patrick O'Farrell for valuable discussions and for communicating unpublished data. We are grateful to Dr. Michael Klymkowsky for advice on immunofluorescence procedures and for the use of his microscope, Dr. Tim Karr for advice on staining embryos, Drs. Susan Dutcher and Michael Klymkowsky for criticizing the manuscript, and Cathy S. Inouye and Karen Brown for secretarial help.

This work was supported by NIH grant #1 RO1 HD18163 to M. P. S. and a Damon Runyon-Walter Winchell Postdoctoral Fellowship #DRG-659 to S. B. C.

The costs of publication of this article were defrayed in part by the payment of page charges. This article must therefore be hereby marked "*advertisement*" in accordance with 18 U.S.C. Section 1734 solely to indicate this fact.

Received July 12, 1985

References

Akam, M. (1983). The location of *Ultrabithorax* transcripts in Drosophila tissue sections. EMBO J. *2*, 2075–2084.

Beachy, P. A., Helfand, S. L., and Hogness, D. S. (1985). Segmental distribution of bithorax complex proteins during Drosophila development. Nature *313*, 545–551.

Carroll, S. B., Riley, P. D., Klymkowsky, M. W., Van Blerkom, J., Stewart, J., and Scott, M. P. (1985). Localization of homoeodomain-containing proteins using antibodies against a synthetic oligopeptide. Symp. Soc. Devel. Biol. *44*, in press.

Crick, F. H. C., and Lawrence, P. A. (1975). Compartments and polyclones in insect development. Science *189*, 340–347.

DiNardo, S., Kuner, J. M., Theis, J., and O'Farrell, P. H. (1985). Development of embryonic pattern in Drosophila melanogaster as revealed by accumulation of the nuclear *engrailed* protein. Cell *43*, this issue.

Foe, V. E., and Alberts, B. M. (1983). Studies of nuclear and cytoplasmic behaviour during the five mitotic cycles that precede gastrulation in *Drosophila* embryogenesis. J. Cell Sci. *61*, 31–70.

Garcia-Bellido, A. (1968). Cell lineage in the wing disc of Drosophila melanogaster. Genetics *60*, 181–193.

Gehring, W. J. (1985). The homeo box: a key to the understanding of development? Cell *40*, 3–5.

Germino, J., Gray, J. G., Charbonneau, H., Vanaman, T., and Bastia, D. (1983). Use of gene fusions and protein–protein interaction in the isolation of a biologically active regulatory protein: the replication initiator protein of plasmid R6K. Proc. Natl. Acad. Sci. USA *80*, 6848–6852.

Hafen, E., Kuroiwa, A., and Gehring, W. J. (1984). Spatial distribution of transcripts from the segmentation gene *fushi tarazu* during Drosophila embryonic development. Cell *37*, 833–841.

Hartenstein, V., and Campos-Ortega, J. A. (1985). Fate-mapping in wild-type Drosophila melanogaster. I. The spatio-temporal pattern of embryonic cell divisions. Roux's Arch. Dev. Biol. *194*, 181–195.

Jürgens, G., Wieschaus, E., Nüsslein-Volhard, C., and Kluding, H. (1984). Mutations affecting the pattern of the larval cuticle in Drosophila melanogaster. II. Zygotic loci on the third chromosome. Wilhelm Roux Arch. *193*, 283–295.

Kaufman, T. C., Lewis, R., and Wakimoto, B. (1980). Cytogenetic analysis of chromosome 3 in Drosophila melanogaster: the homeotic gene complex in polytene chromosome interval 84A,B. Genetics *94*, 115–133.

Kornberg, T. (1981). Compartments in the abdomen of Drosophila and the role of the *engrailed* locus. Dev. Biol. *86*, 363–381.

Kornberg, T., Siden, I., O'Farrell, P., and Simon, M. (1985). The *engrailed* locus of Drosophila: in situ localization of transcripts reveals compartment-specific expression. Cell *40*, 45–53.

Kuroiwa, A., Hafen, E., and Gehring, W. J. (1984). Cloning and transcriptional analysis of the segmentation gene *fushi tarazu* of Drosophila. Cell *37*, 825–831.

Laughon, A., and Scott, M. P. (1984). Sequence of a Drosophila segmentation gene: protein structure homology with DNA-binding proteins. Nature *310*, 25–31.

Lehmann, R., Jimenez, F., Dietrich, U., and Campos-Ortega, J. (1983). On the phenotype and development of mutants of early neurogenesis in Drosophila melanogaster. Roux Arch Dev. Biol. *192*, 62–74.

Levine, M., Hafen, E., Garber, R. L., and Gehring, W. J. (1983). Spatial distribution of *Antennapedia* transcripts during Drosophila development. EMBO J. *2*, 2037–2046.

Lohs-Schardin, M., Cremer, C., and Nüsslein-Volhard, C. (1979). A fate map for the larval epidermis of Drosophila melanogaster: localized cuticle defects following irradiation of the blastoderm with an ultraviolet laser microbeam. Devel. Biol. *73*, 239–255.

Martinez-Arias, A., and Lawrence, P. A. (1985). Parasegments and compartments in the Drosophila embryo. Nature *313*, 639–642.

Mitchison, T. J., and Sedat, J. (1983). Localization of antigenic determinants in whole *Drosophila* embryos. Dev. Biol. *99*, 261–264.

McGinnis, W., Levine, M., Hafen, E., Kuroiwa, A., and Gehring, W. J. (1984). A conserved DNA sequence found in homeotic genes of the Drosophila Antennapedia and bithorax complexes. Nature *308*, 428–433.

Nüsslein-Volhard, C., and Wieschaus, E. (1980). Mutations affecting segment number and polarity in Drosophila. Nature *287*, 795–801.

Nüsslein-Volhard, C., Weischaus, E., and Kluding, H. (1984). Mutations affecting the pattern of the larval cuticle in Drosophila melanogaster. I. Zygotic loci on the second chromosome. Wilhelm Roux Arch. *193*, 267–282.

Poulson, D. F. (1950). Histogenesis, organogenesis, and differentiation in the embryo of Drosophila melanogaster. In Biology of Drosophila, M. Demerec, ed. (New York: Wiley), pp. 168–274.

Sander, K. (1976). Morphogenetic movements in insect embryogenesis. In Insect Development, P. Lawrence, ed. (New York: Halstead Press, Wiley and Sons), pp. 35–52.

Schneider, C., Newman, R. A., Sutherland, D. R., Asser, U., and Greaves, M. F. (1982). A one-step purification of membrane proteins using a high efficiency immunomatrix. J. Biol. Chem. *257*, 10766–10769.

Scott, M. P., and Weiner, A. J. (1984). Structural relationships among genes that control development: sequence homology between the *Antennapedia*, *Ultrabithorax*, and *fushi tarazu* loci of *Drosophila*. Proc. Natl. Acad. Sci. USA *81*, 4115–4119.

Towbin, H., Staehelin, T., and Gordon, J. (1979). Electrophoretic transfer of proteins from polyacrylamide gels to nitrocellulose sheets: procedure and some applications. Proc. Natl. Acad. Sci. USA *76*, 4350–4354.

Turner, F. R., and Mahowald, A. P. (1977). Scanning electron microscopy of *Drosophila melanogaster* embryogenesis: II. Gastrulation and segmentation. Dev. Biol. *57*, 403–416.

Wakimoto, B. T., and Kaufman, T. C. (1981). Analysis of larval segmentation in lethal genotypes associated with the Antennapedia gene complex in Drosophila melanogaster. Dev. Biol. *81*, 51–64.

Wakimoto, B. T., Turner, F. R., and Kaufman, T. C. (1984). Defects in embryogenesis in mutants associated with the Antennapedia gene complex of Drosophila melanogaster. Dev. Biol. *102*, 147–172.

Weber, K., and Osborn, M. (1975). Sodium dodecyl sulfate polyacrylamide gel electrophoresis of proteins. In The Proteins, vol. 1, 3rd Ed., H. Neurath and R. L. Hill, eds. (New York: Academic Press), pp. 179–223.

Weiner, A. J., Scott, M. P., and Kaufman, T. C. (1984). A molecular analysis of *fushi tarazu*, a gene in Drosophila melanogaster that encodes a product affecting embryonic segment number and cell fate. Cell *37*, 843–851.

White, R. A. H., and Wilcox, M. (1984). Protein products of the Bithorax Complex in Drosophila. Cell *39*, 163–171.

Wieschaus, E., Nüsslein-Volhard, C., and Jurgens, G. (1984). Mutations affecting the pattern of the larval cuticle in Drosophila melanogaster. III. Zygotic loci on the X chromosome and fourth chromosome. Wilhelm Roux Arch. *193*, 296–307.

Young, R. A., and Davis, R. W. (1983). Efficient isolation of genes by using antibody probes. Proc. Natl. Acad. Sci. USA *80*, 1194–1198.